Physica E 93 (2017) 124–131

Contents lists available at ScienceDirect

Physica E

journal homepage: www.elsevier.com/locate/physe

Length and temperature dependence of the mechanical properties of finite-size carbyne

Xueming Yang[a,b,*], Yanhui Huang[b], Bingyang Cao[a,**], Albert C. To[c]

[a] Key Laboratory for Thermal Science and Power Engineering of Ministry of Education, Department of Engineering Mechanics, Tsinghua University, Beijing 100084, China
[b] Department of Power Engineering, North China Electric Power University, Baoding 071003, China
[c] Department of Mechanical Engineering and Materials Science, University of Pittsburgh, PA 15260, USA

ABSTRACT

Carbyne is an ideal one-dimensional conductor and the thinnest interconnection in an ultimate nano-device and it requires an understanding of the mechanical properties that affect device performance and reliability. Here, we report the mechanical properties of finite-size carbyne, obtained by a molecular dynamics simulation study based on the adaptive intermolecular reactive empirical bond order potential. To avoid confusion in assigning the effective cross-sectional area of carbyne, the value of the effective cross-sectional area of carbyne (4.148 Å^2) was deduced via experiment and adopted in our study. Ends-constraints effects on the ultimate stress (maximum force) of the carbyne chains are investigated, revealing that the molecular dynamics simulation results agree very well with the experimental results. The ultimate strength, Young's Modulus and maximum strain of carbyne are rather sensitive to the temperature and all decrease with the temperature. Opposite tendencies of the length dependence of the overall ultimate strength and maximum strain of carbyne at room temperature and very low temperature have been found, and analyses show that this originates in the ends effect of carbyne.

1. Introduction

The single carbon atom chain (SCC) carbyne has been regarded as an ideal one-dimensional conductor and is the thinnest interconnection possible for an ultimate nano-device. Hence, carbynes may be applied in future devices such as transport channels, on-chip interconnects for molecular electronics, and spintronic nano-devices. The existence of carbyne chains has recently been demonstrated through experimental observation [1–7] and measurements [8–13], and studies have shown that SCCs can be synthesized by techniques such as unraveling a nanotube [8,13] or shrinking a carbon nanotube [2,4,9], forming SCC inside a carbon nanotube [5,12], deriving carbon atomic chains from graphene or ultra-narrow graphene nanoribbons [3,6,7], and coalescence of functionalized fullerenes filled into a single-wall carbon nanotube [1].

The application of carbyne in different devices will likely require a deeper understanding of its mechanical properties, which would affect device performance and reliability. The results of both experimental and theoretical studies of the mechanical properties of carbyne are compared and the results are listed in Table 1. Recent experimental studies [14–16] have shown that carbyne is stronger than any known material. Mikhailovskij et al. [14] reported an ultimate strength of 270 GPa (11.2 nN) of carbyne at 5 K via field-ion microscope (FIM) in which the ultimate strength can be measured without the requirement to assign an effective cross-sectional area on which the force is applied. Kotrechko et al. [15] reported an ultimate strength of 251 GPa of carbyne at 77 K using FIM for experimental measurement of carbyne strength.

A comprehensive understanding of the dependence of the mechanical properties of carbyne on length and temperature through an experimental study alone remains challenging, and thus theoretical study is necessary and helpful. Although there are a few theoretical studies on the mechanical behavior of carbyne, published results seem contradictory. Nair et al. [17] reported the mechanical properties of carbyne, obtained by first-principles–based ReaxFF molecular simulation. They reported a Young's modulus of 288 GPa and a strength that ranges from 11 GPa (1.3 nN) for the shortest length to a constant 8 GPa (0.9 nN) for lengths of 5–64 Å. However, in another study that

* Corresponding author at: Key Laboratory for Thermal Science and Power Engineering of Ministry of Education, Department of Engineering Mechanics, Tsinghua University, Beijing 100084, China.
** Corresponding author.
E-mail addresses: ncepub@hotmail.com (X. Yang), caoby@tsinghua.edu.cn (B. Cao).

http://dx.doi.org/10.1016/j.physe.2017.06.006
Received 13 September 2016; Received in revised form 26 March 2017; Accepted 3 June 2017
Available online 04 June 2017

Table 1
Comparing the mechanical properties of carbyne.

Method	Temperature (K)	Thickness (h) or diameter (d) (Å)	Cross section area (Å^2)	Maximum tensile force (nN)	Young's modulus (TPa)	Ultimate strength (Gpa)
DFT [18]		d=0.772	0.4681	9.3–11.7	32.71	1986.8–2499.5
ReaxFF molecular simulation [17]	10	h=3.35	11.2225	0.9–1.3	0.288	8–11
Experiment (FIM) [14]	5			11.2		270
Experiment (FIM) [15]	77	d=2.0	3.1416	7.85 ± 0.05		251
Ab initio calculation [15]	0	d=2.0	3.1416	10.2–13.09	3.48–4.63	324–417
ReaxFF molecular simulation [19]	500	d=3.35	8.8141	7.53	1.345	67.1
ReaxFF molecular simulation [20]	100–400			8.75–9.75		
Experiment (FIM) [16]		d=2.0	3.1416	7.916		252.1

utilized first-principles calculations by Liu et al. [18], the reported Young's modulus (32.7 TPa) and strength (9.3–11.7 nN) of the carbyne are much higher than the results reported by A. K. Nair et al. However, in their study, the very high Young's modulus of 32.71 TPa and the specific strength of 6.0–7.5 × 10^7 Nm/kg seem to result from using an effective mechanical thickness of 0.772 Å, which is much smaller compared to the graphite interlayer spacing of 0.335 nm by convention. Liu et al. [19] and Mirzaeifar et al. [20] also investigated the mechanical behavior of carbyne, using the ReaxFF molecular simulation, and their results are inconsistent with the results of the above theoretical studies with or without considering the influence of a cross section area.

In this study, we investigate the mechanical properties of carbyne, using molecular dynamic (MD) simulations in combination with the Adaptive Intermolecular Reactive Empirical Bond Order (AIREBO) potential [21]. By using the effective cross-sectional area of carbyne, which we deduced from experiment, the results of MD simulations based on AIREBO potential are compared and validated with experimental results. Then, the length dependence and temperature dependence of mechanical properties of carbyne, specifically the ultimate strength and the Young's Modulus and maximum strain of carbyne, are investigated in detail.

Isolated single carbon atom chains that include more than 20 atoms have been reported to be energetically unstable [12,22–24]. Recent studies have shown that the nanoscale confinements or end constrains are a necessary condition for stabilizing the long SCCs [12,25–27], and similar to carbon nanotubes (CNTs) and graphene nanoribbons (GNRs), the physical characteristics of finite carbynes may considerably differ from those of their infinite counterparts [28]. Therefore, our study will only focus on the mechanical properties of finite-size carbyne with end constrains.

2. Computational methods

MD simulations are necessary for the investigation of the mechanical properties of carbyne, as shown in the MD simulations studies on carbyne in the published literature [16,17,19,20]. More importantly, it can be extended to analyze carbyne in more complex environments or with complex constraints [12,20,25–27]. Considering that carbyne a simple single crystal, some theoretical analytic models have been proposed that can provide an approximation of the mechanical properties of carbyne. However, the parameters in these models have to be estimated via simulations results [20,29].

MD simulations are carried out using the LAMMPS package [30] with the AIREBO potential. This potential has been shown to accurately capture the bond–bond interaction between carbon atoms as well as both bond breaking and bond-reforming, and has been widely applied to study the mechanical properties of carbon-based nanostructures [31–36]. In addition, the Brenner potential [37], the REBO potential [38,39], and the AIREBO potential have already been used to model the mechanical behavior of carbyne [25,26,32] and graphynes, in which carbon hexagons are connected via linear carbon chains [40–43]. The function $f_c(r)$ in the REBO part of the AIREBO potential represents the cutoff function that decreases monotonously from 1 to 0 as in

$$f_c(r) = \begin{cases} 1, & r < R_{\min} \\ \left\{1 + \cos\left[\frac{\pi(r - R_{\min})}{R_{\max} - R_{\min}}\right]\right\}/2, & R_{\min} \le r \le R_{\max} \\ 0, & r > R_{\max} \end{cases} \quad (1)$$

where $R_{\min}$ = 1.7 Å and $R_{\max}$ = 2.0 Å in the original AIREBO potential [38,44]. However, the authors of both the Brenner potential and the REBO potential have mentioned that such a value of the parameter $R_{\min}$ in the cutoff function will lead to spuriously high bond forces without a physical basis, since C-C bonds are stretched beyond 1.7 Å. Thus, they suggested that the cutoff distance $R_{\min}$ should be extended far beyond the inflection point [45]. Following their suggestions, larger cutoff distances $R_{\min}$, such as 1.9 Å [46], 1.92 Å [47,48], and 2.0 Å [29,49–53] were employed. Among these, a value of 2.0 Å was the most commonly used in publications, which can avoid the camelback in the potential due to the cutoff function. Such a modified AIREBO potential has been reported to provide a more accurate approximation for the near fracture region [29,45,49–53]. Therefore, the cutoff parameters $R_{\min}$ of the potential are set as 2.0 Å in our simulations.

The (nominal) strain and the engineering (nominal) stress in the x direction are defined as

$$\varepsilon_x = \frac{l_x - l_x^0}{l_x^0}, \quad \sigma_x = \frac{1}{V^0}\frac{\partial U}{\partial \varepsilon_x} \quad (2)$$

where l_x^0 is the initial length of the carbyne in x (i.e. longitudinal) direction at zero strain, l_x is the strained length of the carbyne, U is the strain energy, $V^0 = l_x^0 S$ is the initial volume of the structure, and S is the effective cross-sectional area of the carbyne onto which the tensile force is applied. The Young's modulus Y in x direction is defined via the equation:

$$Y = \frac{1}{V^0}\frac{\partial^2 U}{\partial \varepsilon_x^2}\bigg|_{\varepsilon_x = 0} \quad (3)$$

The atomic models of an isolated carbyne chain are displayed in Fig. 1. Theoretically, stable carbon chain structures may be double-bonded (polycumulene), $[=(=\ C\ =)\ =]_n$ or alternating single-triple bonded (polyyne), $[-(-C \equiv C-)-]_n$. In our simulations, the single/triple/double bond lengths are set as 1.24, 1.34, and 1.284 Å [43,54–57], respectively. Since it has been reported that carbon chains are always subject to a time-varying nonzero strain that transforms their atomic structure from cumulene to polyyne configuration [11], and recent experimental studies have confirmed that carbyne exists in a stable polyyne structure and could thus be synthesized [17], our simulations only focus on polyyne chains. Finite-length carbynes

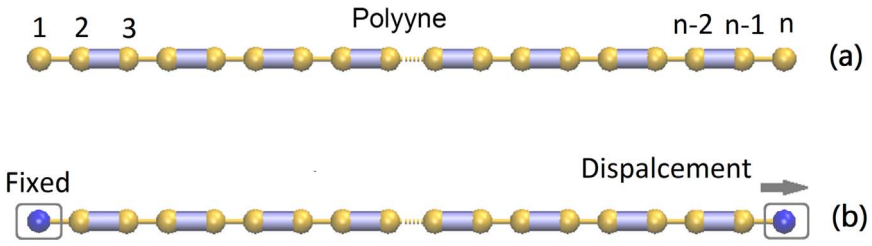

Fig. 1. Isolated carbyne chains used for simulation.

without constraints are unstable and flexible due to fluctuations induced by temperature, and thus before applying tension, finite-length carbynes are first energy-minimized; then, the atoms at the ends are fixed and are equilibrated at simulation temperature to ensure structural stability.

In each MD simulation of the tensile loading process, the optimal scheme 2 (S2) is employed, as previously described [58]. The first atom in the carbyne is fixed, and a displacement step is applied on the last atom, which is held rigid. All atoms except the end atoms are attached to the Nosé–Hoover thermostat during the loading process. Each displacement step is followed by 1000 relaxation steps, and the simulation time step is set to be 0.5 fs. The strain rates vary with carbyne length in the range from 1.0×10^8 s^{-1} to 2×10^8 s^{-1}, which is in agreement with strain rates selected in Ref. [59].

One important issue should be noted in the calculation of the ultimate strength and the Young's modulus is the determination of the cross section area of the carbyne. Similar to the well-known "Yakobson's paradox" which refers to the contradicting values of the Young's modulus of CNT as reported in previous literature due to the non-unique definition of the thickness of single-wall CNTs [60,61], the assumption of the effective cross-sectional area of carbyne is also confusing when calculating the ultimate strength and Young's modulus of carbyne. As shown in Table 1, the scattered mechanical properties of carbyne are partially caused by differing assumptions. Nair et al. [17] used an effective cross-sectional area value of 3.35×3.35 $Å^2$. Liu et al. [19] used a diameter of the carbyne chain of 3.35 Å, which corresponds to an effective cross-sectional area of 8.8141 $Å^2$ and is similar to a previously utilized approach for defining the cross section of graphene and carbon nanotubes [62–64]. Kotrechko et al. [15] and Mazilova et al. [16] used a diameter of a carbyne chain of 2.0 Å (or an effective cross-sectional area of 3.1416 $Å^2$), which is the cutoff distance of the Tersoff–Brenner bond-order potential.

Although Yakobson's group [18] have previously determined a mechanical radius of 0.386 Å, using the equivalent continuum mechanics model, their obtained mechanical radius is questionable. Moreover, the problem of determining the cross-sectional area has not been solved unequivocally. (1) Their results showed a fracture force of carbyne of 9.3–11.7 nN and a derived mechanical radius of 0.386 Å. Thus, their ultimate stress can be obtained as 1986.8–2499.5 GPa, which is almost 7–9 times higher than the experimental results (270 GPa). Such results cannot agree with experimental results. (2) Similarly, they have derived a much smaller value of the wall thickness of 0.66 Å in the case of SWNT's, using the continuum mechanics model, which is only one fifth of the commonly adopted thickness of 3.4 Å. Furthermore, their calculated Young's modulus if 5.5 TPa is much higher than the commonly adopted value obtained via experimental results of ~1 Tpa [65].

We noticed that Mikhailovskij et al. [14] have reported an ultimate strength of 270 GPa, which corresponds to a fracture force of 11.2 nN for carbyne at 5 K via FIM. The FIM has a unique advantage that renders it capable of measuring the ultimate strength without the need to assign an effective cross-sectional area onto which the force is applied. Moreover, providing the effective cross-sectional area of the carbyne is not necessary to obtain the fracture force. It should be noted that the apex radius of the emitter, ρ, had to be determined for their measurement via FIM. How the radius ρ was determined has been described in detail in previous publications [14,15], coinciding with the distance between the electric surface and the atomic nucleus at the end of the chain, which was taken equal to 1.2 Å. Using the ratio of the fracture force to the corresponding ultimate strength, we obtain a value of effective cross-sectional area of carbyne of 4.148 $Å^2$, corresponding to a chain diameter of 2.3 Å, which we adopted in our study. Such a deduced value of chain diameter is acceptable when referring to estimated results of effective cross-sectional area via a previously described all-electron Linearised Augmented Plane Wave (LAPW) method [66]. In fact, this value is higher than 2 Å, which has been considered to provide a lower estimate for the carbyne diameter [66], and it is close to the diameter of electrical surfaces for the hemispherical cap of the chain, which are assumed equal to 2.4 Å [14]. Identical to those in the literature [15,66,67], here we choose the maximum stress of 270 GPa at the chain tip rather than the average stress of 245 GPa acting at the chain cap approximated by a hemisphere as measured value of the ultimate strength of the carbyne in Ref. [14].

3. Validation of the methods

To test whether the AIREBO potential can appropriately describe the mechanical properties of carbyne, MD simulations based on the potential for three carbyne chains, consisting of 28 atoms with different end constraints (see Fig. 2(a)) are carried out. Chain A is an isolated carbyne chain. Chain B is set according to the atomic model for a self-standing linear atomic chain, anchored at the graphite tip in FIM [14]. Chain C is modeled as a carbyne chain, constrained by two graphene nanoribbons with 10 layers on each side, which is similar to a previously described atomic model [3]. Similar to simulations of the isolated carbyne chain mentioned above for Chain B and Chain C, the system including both graphene nanoribbons and the carbyne chain is first energy minimized and then atoms of the graphene edge layers at two ends of the system are fixed. The system is equilibrated at the simulation temperature to ensure structural stability. Then, the atoms of the left-edge layer of the system are fixed, and the displacement step is applied on atoms of the right edge layer of the system, which is held rigid. The atoms next to the edge layers are attached to the Nosé–Hoover thermostat in the MD simulations of the loading process.

The obtained results of the stress-strain curves for Chain A, Chain B, and Chain C at a temperature of 77 K are shown in Fig. 2(b). The ultimate stresses (maximum force) are: 240.2052 GPa (9.9637 nN), 230.3117 GPa (9.5533 nN), and 218.3706 GPa (9.058 nN) for Chain A, Chain B, and Chain C, respectively. The ultimate stress of Chain B agrees very well with the experimental result (251 GPa), and the difference may only be caused by the atom number of the measured chains in the experiment of FIM not being exactly 28, as mentioned in Ref. [15]. The measured chains have a mean value of 3.5 nm with a variance of 1.8 nm.

Moreover, we can observe that the ultimate stresses (the maximum force) are related with end constraints of the carbyne chains. The isolated carbyne chain with fixed ends has maximal strength, and the

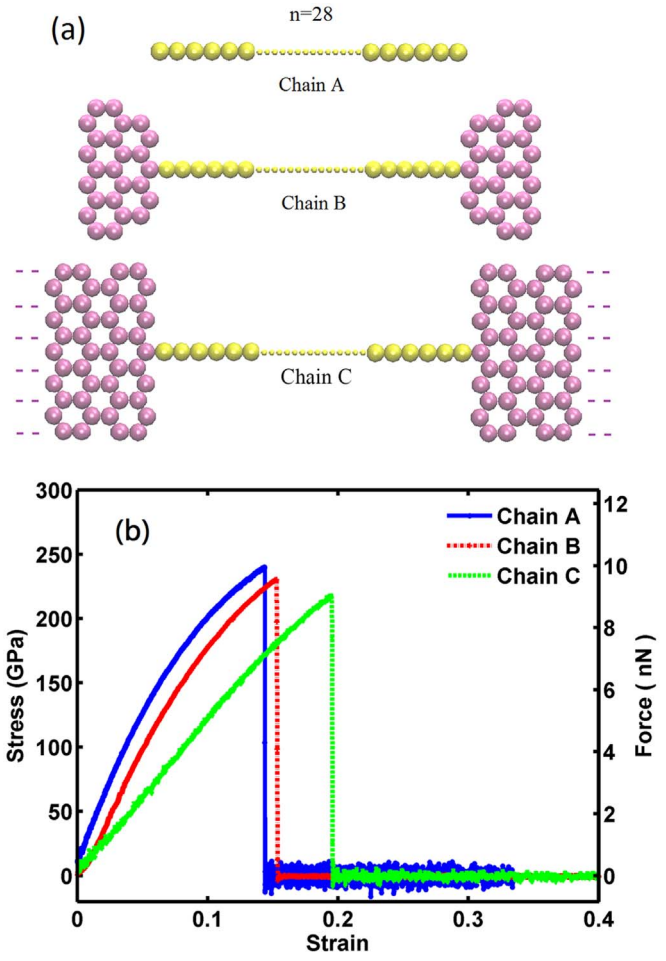

Fig. 2. Strain v.s. stress curves for 3 chain models with different ends constraints: (a) 3 at. models; (b) Strain v.s. stress curves for 3 carbyne chains.

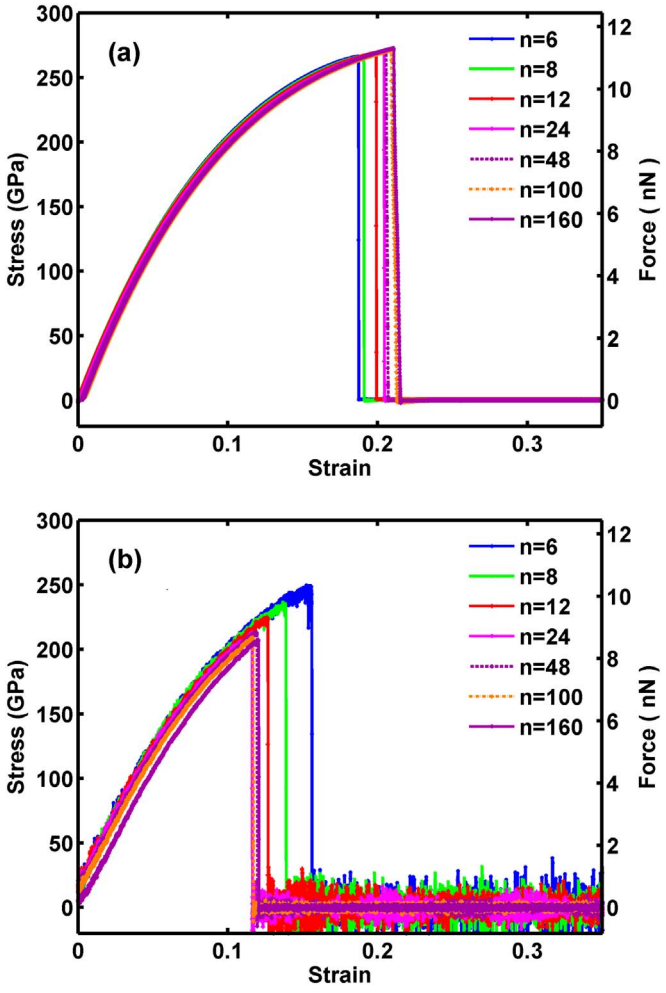

Fig. 3. Stress-strain curves of polyyne chains with different lengths under tensile loading: (a) at temperature of 0.1 K; (b) at temperature of 300 K.

carbyne chain anchored at the rectangular graphene nanoribbon has minimal strength due to the increased stress concentration between chain and graphene.

4. Results and discussion

To investigate the length dependence and the temperature dependence of the mechanical properties of carbyne, polyyne chains of varying lengths, containing n (n = 6, 8, 12, 24, 48, 100, and 160) atoms are generated as shown in Fig. 1(a) and (b), respectively. A series of MD simulations are conducted for the polyyne chains of various lengths at temperatures of 0.1 K, 10 K, and 300 K. Fig. 3(a) and (b) show the stress-strain curves of polyyne chains with different lengths under tensile loading at temperatures of 0.1 K and 300 K, respectively. Relevant results are also expressed in terms of force. The polyyne chains exhibit nonlinear elastic behavior under uniaxial tension, and their ultimate tensile strength and fracture strain strongly depend on their length and temperature. In following section, we will discuss the ultimate tensile strength, fracture strain, and the Young's modulus of the polyyne chains obtained from the stress–strain curves.

4.1. Length dependence and temperature dependence of the ultimate strength and maximum strain of carbyne

Throughout previous studies [15,17], the results of the length dependence of mechanical properties of carbyne have been reported. Kotrechko et al. [15] reported results obtained via *ab initio* simulations, showing that the strength of chains with an even number of atoms increases with the number of atoms n, when n is in the range of 2–12, and when n > 12, the strength becomes independent of the chain length. However, ReaxFF molecular simulations study by Nair [17] have shown that the strength of carbynes decreases with the number of atoms before it reaches an asymptotic value as the chain length approaches ~60 Å. Therefore, the underlying reason for this difference in length dependence should be further investigated and clarified.

Fig. 4 shows a different trend at different temperatures for the length dependence of the ultimate strength and maximum strain of carbyne. At 10 K and 300 K, the ultimate strength and maximum strain both first decrease with the number of atoms of the chain, then gradually becoming independent of chain length, which is in agreement with the results of MD simulations in Ref. [20]. However, the length dependence of the ultimate strength and maximum strain of carbyne shows a reverse trend at a very low temperature of 0.1 K. Both ultimate strength and maximum strain increase with the number of chain atoms until they reach an asymptotic value, which is in agreement with the results of previously published *ab initio* calculations [15]. Consequently, we have found opposite tendencies for the length dependence of the overall ultimate strength and maximum strain of carbyne at room temperature and very low temperature approaching 0 K.

In the following, we will discuss the difference in the behavior of length dependence shown above. Mirzaeifar et al. [20] proposed a theoretical equation to describe the length dependence and temperature dependence of the ultimate stress of carbyne as follows:

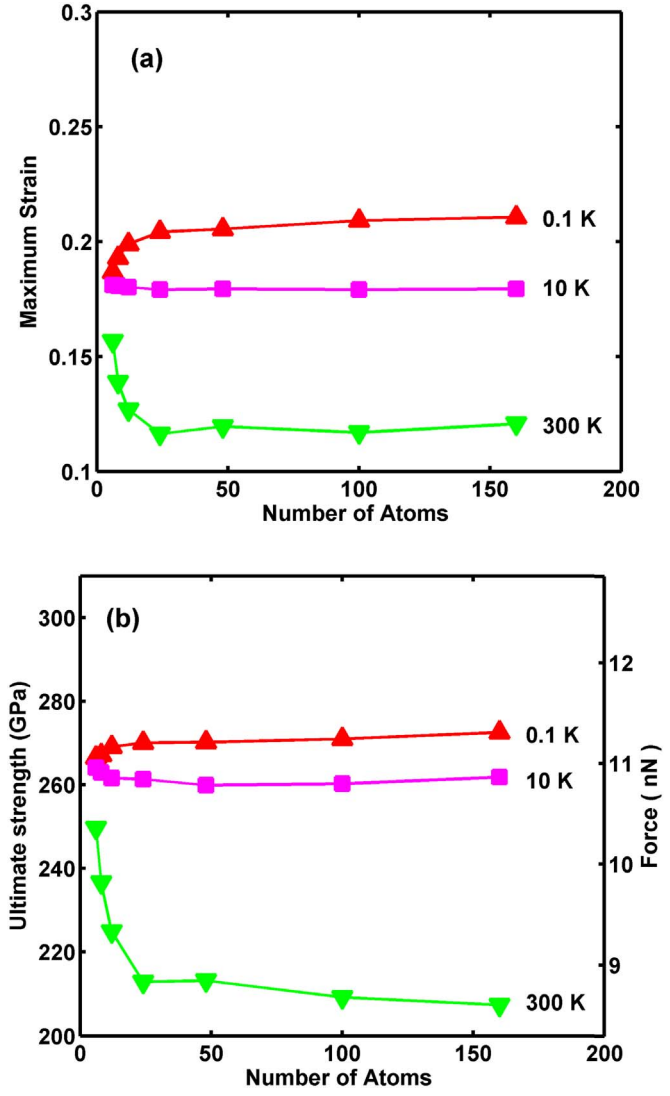

Fig. 4. Length dependence curve of the overall maximum strain and ultimate strength of polyyne chains (a) maximum strain; (b) ultimate strength.

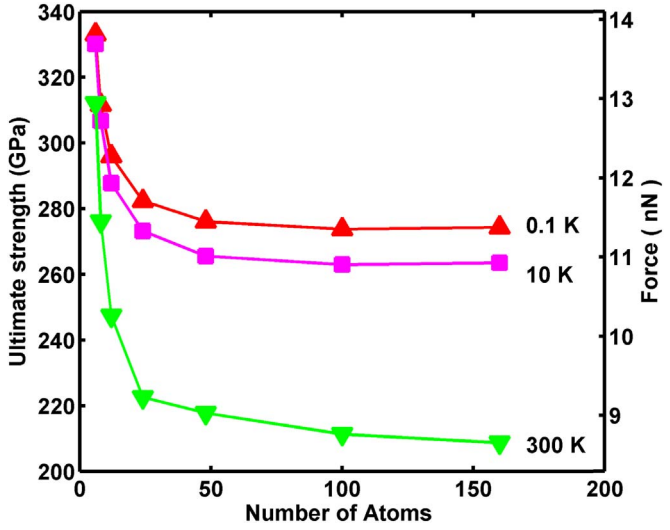

Fig. 5. Length dependence curve of ultimate strength of free atoms in the polyyne chains.

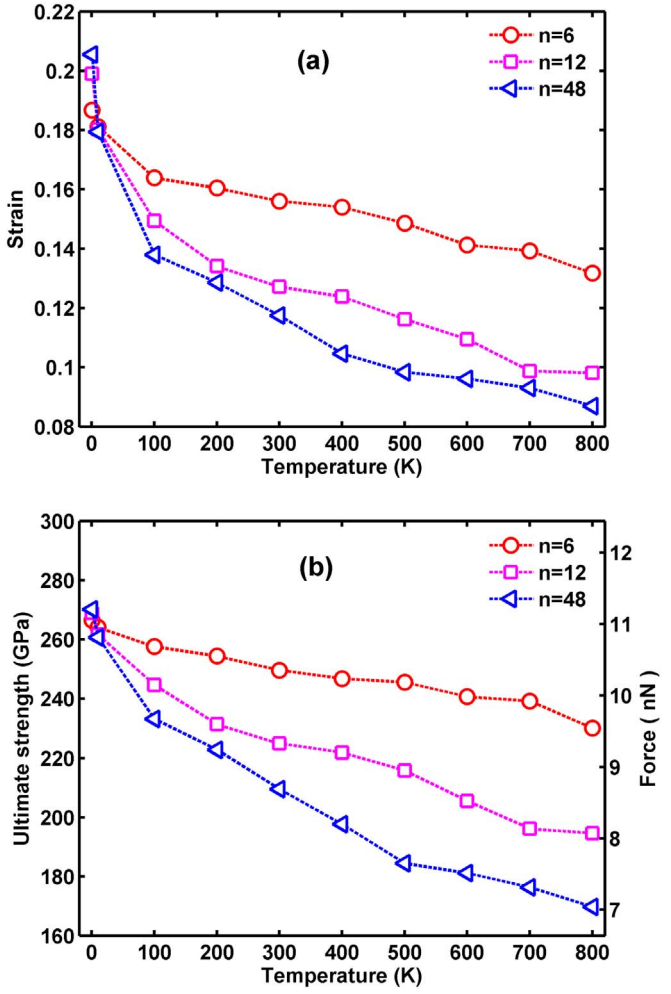

Fig. 6. Temperature dependence curve of maximum strain and ultimate strength of polyyne chains (a) maximum strain; (b) ultimate strength.

$$\sigma_r = \frac{k_B T}{x_{b1} A} \ln\left(\frac{2v}{\omega_1 N^a x_b}\right) + \frac{E_{b1}}{x_{b1} A} \tag{4}$$

where N is the total number of bonds in the carbyne, T is the temperature, a is the power factor from the extended Bell model, x_{b1} is the separation distances of single CC bonds in the carbyne chain, A is the cross section area of the carbyne chain, ω_1 are the natural vibration frequencies of single CC bonds, E_{b1} are the energies of single CC bonds, and k_B is the Boltzmann constant. However, it seems that Eq. (4) is not fitting the MD simulation results very well that are based on the ReaxFF potential, especially for carbyne chains with small length or at low temperatures. Moreover, Eq. (4) reveals that σ_r decreases with N for any given T. Thus, Eq. (4) cannot explain why σ_r increases with N at very low temperatures. Additionally, both our results and those in a previous study [17] for length dependence of the ultimate strength, show a much faster convergence than the results obtained with Eq. (4). Furthermore, they more likely obey exponential damping law with the length.

Considering an analytical expression for the nonlinear elastic (NLE) behavior of carbyne under uniaxial tension as follows [29]:

$$\sigma_r(N, T) = \frac{a k_B T}{\gamma a + k_B T}\left\{\frac{U_0}{k_B T} + \ln\left[\frac{b\dot{\varepsilon}\tau_0}{N}\left(\frac{\gamma a}{k_B T} + 1\right)\right]\right\} \tag{5}$$

where U_0 is the interatomic bond dissociation energy, and $\gamma = qV$, where V is the activation volume and q is the coefficient of local overstress, k_B is the Boltzmann constant, $\dot{\varepsilon}$ is the strain rate, and τ_0 is the vibration period of

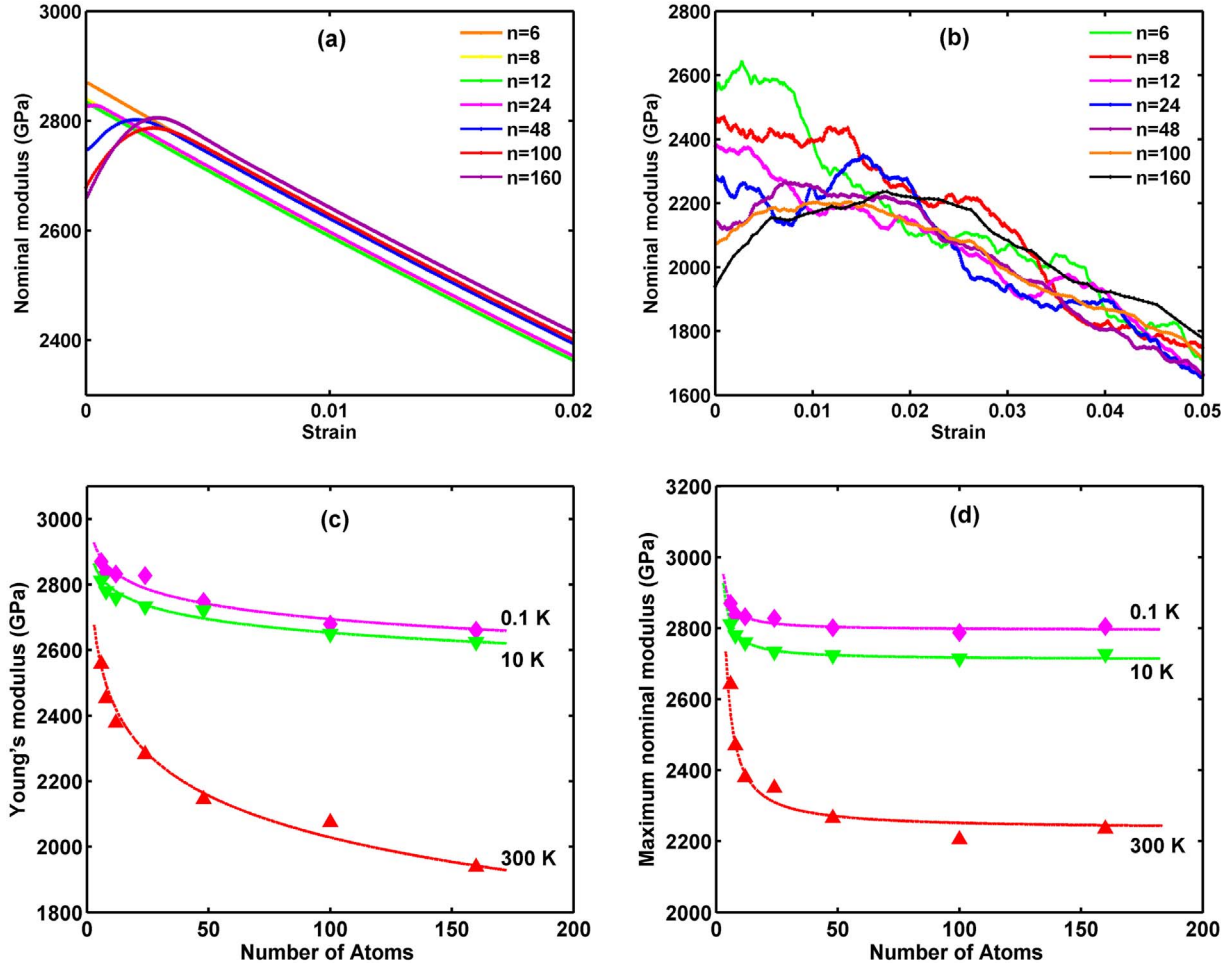

Fig. 7. Length dependence of Young's modulus and the maximum nominal modulus of carbyne (a) nominal modulus of polyyne chains with varied length at 0.1 K; (b) nominal modulus of polyyne chains with varied length at 300 K; (c) Length dependence of Young's modulus; (d) Length dependence of the maximum nominal modulus.

atoms in solids. Eq. (5) reveals that σ_r will also decrease with N for any given T.

Thus, the above discussions show that the theoretical models for analysis via Eqs. (4) and (5) cannot explain why σ_r increases with N at temperatures approaching 0 K, which has been observed in the *ab initio* calculations [15]. In fact, although Eqs. (4) and (5) are helpful to understand the length dependence of the ultimate strength of carbyne, some of their parameters have to be estimated from MD simulations.

To explain the opposite tendency of length dependence of the ultimate strength and maximum strain of carbyne shown at room temperature and very low temperature, we separately calculated the ultimate stress and maximum strain of carbyne for fixed atoms at the ends and for free atoms in the middle. We found that the stress of the fixed atom is much less than that of the free atom, thus resulting in an overall ultimate stress that is smaller than the ultimate stress calculated for free atoms. Such an end effect is much stronger for shorter carbyne chains. The ultimate stresses for free atoms are compared and shown in Fig. 5. The trends of length dependence of ultimate stresses for free atoms become identical for very low temperatures and for room temperature. Also, similar to the length dependence of the overall ultimate strength and maximum strain, the values of ultimate stresses follow an exponential damping law with length rather than logarithm damping law with length, which can be obtained using Eqs. (4) and (5). Therefore, we demonstrate that the different length dependence at both room temperature and very low temperatures may be the result of the end effect caused by the end atoms.

A further question is whether such an end effect should be eliminated or whether periodic boundary conditions should be used. To answer this question, we would also like to remind that we are dealing with finite systems here. Although periodic boundary conditions were applied in the tensile direction in some previous MD simulations studies to remove the finite length effect, the size effects and end effects are real material effects in nanoscale and not simply an artifact. When we focus on the finite size effect of properties of a finite nanomaterial system, it is apparent that both size effect and end effects should not be eliminated, and the free boundary condition is more natural than the periodic boundary conditions [28,68–70].

As shown in Fig. 6, the ultimate strength and maximum strain of polyyne chains decrease almost linearly with temperature, except at temperatures below 100 K. The temperature dependence of the ultimate strength agrees with previously published ReaxFF molecular simulation results [20], and it can be also observed that Eq. (4) cannot linear fit their MD results for temperatures below 100 K. The temperature dependence of the maximum strain corresponds well with the theoretical prediction for graphene nanoribbons with a fracture strain that decreases almost linearly with increasing temperature except at temperatures below 90 K [64].

4.2. Length dependence of the Young's Modulus of carbyne

The carbyne chains will become softer when either temperature or length increases. Fig. 7(a) and (b) show the nominal modulus as a function of the strain ε for polyyne chains of various lengths at 0.1 K and 300 K, respectively. To be consistent with the calculated value of the Young's modulus, the nominal moduli at strain ε are calculated via differentiating the stress with respect to the strain in a range of ε~ε +

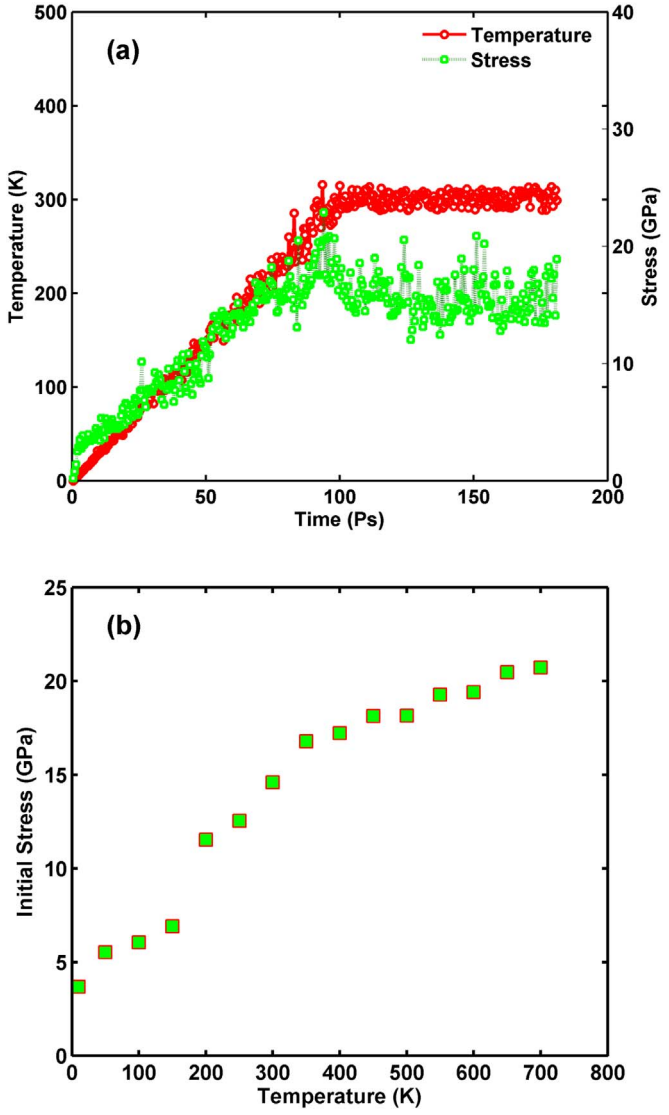

Fig. 8. Initial stress of the carbyne chains before the tensile process start. (a) stress variation in the heating and equilibration process; (b) temperature- initial curve of the carbyne chain.

0.02, and the Young's moduli of carbyne is obtained from the stress-strain data acquired via the Hooke's law $\sigma = E\varepsilon$ at a small strain level ($\varepsilon \leq 0.02$). Fig. 7(c) and (d) show the Young's modulus and the maximum nominal modulus as a function of strain ε for polyyne chains of different lengths at different temperatures, respectively. The Young's modulus of carbyne obeys a logarithmic damping law with length, while the maximum nominal modulus of carbyne follows a modified exponential damping law with lengths. Furthermore, both the Young's modulus and the maximum nominal modulus decrease with increasing temperature.

4.3. Initial stress of carbyne

Carbyne chains are much more flexible and unstable than other carbon nanostructures, such as graphene and carbon nanotubes. Finite size carbyne chains under the free boundary condition show apparent fluctuations when temperatures are non-zero. Even their ends atoms are fixed, and these temperature induced fluctuations will result in initial stress in the carbyne chains before the start of the tensile process, and this can explain that the initial stress value in Fig. 3(b) is not zero. To obtain the tensile behavior of a carbyne system at a given simulation temperature T in MD simulations, a temperature control process is necessary before loading, in which the temperature of the system (except for the atoms at both ends) is tuned to T. To do so, the temperature of the system linearly increases from 0 K to T in 100 ps. Then, the system is equilibrated at the simulation temperature for 80 ps with temperature control (NVT ensemble), and the stresses in the last 20 ps of the equilibration are averaged as the initial stress before loading. Fig. 8(a) shows how the stress of a carbyne chain with 12 atoms varies with instantaneous temperature in the temperature control process before loading when the simulation temperature of T = 300 K. It can be observed that the stress almost increases with the instantaneous temperature. Fig. 8(b) shows that the initial stress steadily increases with the simulation temperature and the rate of increase slows down as the temperature surpasses 350 K.

5. Conclusions

Carbyne is the thinnest carbon nanostructure and thus has important potential applications in future nanodevices. To understand the mechanical properties of carbyne, MD simulations employing the AIREBO potential are conducted in this study to investigate the Young's Modulus, the ultimate strength, and the maximum strain of carbyne as well as their length dependence and temperature dependences.

MD simulations with AIREBO potential are conducted and results are compared with experimental results. MD simulations with AIREBO potential can well describe the mechanical properties of carbyne. Furthermore, the mechanical properties of carbyne, such as the ultimate strength and the Young's Modulus, are better by a factor of 2 compared to graphene and carbon nanotubes when assigning the experimentally deduced effective cross-sectional area. The ultimate strength, Young's Modulus and maximum strain of carbyne are rather sensitive to temperature, and almost all decrease linearly with temperature. Opposite tendencies of the length dependence of the overall ultimate strength and maximum strain of carbyne at room temperature and at very low temperatures are found, and the results reveal this as a result of the end effect of the carbyne.

Acknowledgments

This research is supported by the National Natural Science Foundation of China (Grant Nos. 51576066, 51322603, 51136001 and 51356001), the Natural Science Foundation of Hebei Province of China (Grant No. E2014502042) and the China Postdoctoral Science Foundation (Grant No. 2015M570095).

References

[1] F. Boerrnert, C. Boerrnert, S. Gorantla, X.J. Liu, A. Bachmatiuk, J.-O. Joswig, F.R. Wagner, F. Schäffel, J.H. Warner, R. Schönfelder, B. Rellinghaus, T. Gemming, J. Thomas, M. Knupfer, B. Büchner, M.H. Rümmeli, Single-wall-carbon-nanotube/single-carbon-chain molecular junctions, J. Phys. Chem. B 81 (2010) 085439.
[2] H.E. Troiani, M. Miki-Yoshida, G.A. Camacho-Bragado, M.A.L. Marques, A. Rubio, J.A. Ascencio, M. Jose-Yacaman, Direct observation of the mechanical properties of single-walled carbon nanotubes and their junctions at the atomic level, Nano Lett. 3 (2003) 751–755.
[3] C. Jin, H. Lan, L. Peng, K. Suenaga, S. Iijima, Deriving carbon atomic chains from graphene, Phys. Rev. Lett. 102 (2009) 205501.
[4] G. Casillas, A. Mayoral, M. Liu, A. Ponce, V.I. Artyukhov, B.I. Yakobson, M. Jose-Yacaman, New insights into the properties and interactions of carbon chains as revealed by HRTEM and DFT analysis, Carbon 66 (2014) 436–441.
[5] Z. Wang, X. Ke, Z. Zhu, F. Zhang, M. Ruan, J. Yang, Carbon-atom chain formation in the core of nanotubes, Phys. Rev. B 61 (2000) 2472.
[6] J.C. Meyer, C.O. Girit, M.F. Crommie, A. Zettl, Imaging and dynamics of light atoms and molecules on graphene, Nature 454 (2008) 319–322.
[7] A. Chuvilin, J.C. Meyer, G. Algara-Siller, U. Kaiser, From graphene constrictions to single carbon chains, New J. Phys. 11 (2009) 083019.
[8] A.G. Rinzler, J.H. Hafner, P. Nikolaev, P. Nordlander, D.T. Colbert, R.E. Smalley, L. Lou, S.G. Kim, D. Tománek, Unraveling nanotubes: field emission from an atomic wire, Science 269 (1995) 1550.
[9] T.D. Yuzvinsky, W. Mickelson, S. Aloni, G.E. Begtrup, A. Kis, A. Zettl, Shrinking a carbon nanotube, Nano Lett. 6 (2006) 2718–2722.

[10] C. Fantini, E. Cruz, A. Jorio, M. Terrones, H. Terrones, G. Van Lier, J.-C. Charlier, M.S. Dresselhaus, R. Saito, Y.A. Kim, T. Hayashi, H. Muramatsu, M. Endo, M.A. Pimenta, Resonance Raman study of linear carbon chains formed by the heat treatment of double-wall carbon nanotubes, Phys. Rev. B 73 (2006) 3408.
[11] O. Cretu, A.R. Botello-Mendez, I. Janowska, C. Pham-Huu, J.-C. Charlier, F. Banhart, Electrical transport measured in atomic carbon chains, Nano Lett. 13 (2013) 3487–3493.
[12] X. Zhao, Y. Ando, Y. Liu, M. Jinno, T. Suzuki, Carbon nanowire made of a long linear carbon chain inserted inside a multiwalled carbon nanotube, Phys. Rev. Lett. 90 (2003) 187401.
[13] M.A.L. Marques, H.E. Troiani, M. Miki-Yoshida, M. Jose-Yacaman, A. Rubio, On the breaking of carbon nanotubes under tension, Nano Lett. 4 (2004) 811–815.
[14] I.M. Mikhailovskij, E.V. Sadanov, S. Kotrechko, V.A. Ksenofontov, T.I. Mazilova, Measurement of the inherent strength of carbon atomic chains, Phys. Rev. B 87 (2013) 045410.
[15] S. Kotrechko, I. Mikhailovskij, T. Mazilova, E. Sadanov, A. Timoshevskii, N. Stetsenko, Y. Matviychuk, Mechanical properties of carbyne: experiment and simulations, Nanoscale Res. Lett. 10 (2015) 1–6.
[16] T.I. Mazilova, S. Kotrechko, E.V. Sadanov, V.A. Ksenofontov, I.M. Mikhailovskij, High-field formation of linear carbon chains and atomic clusters, Int. J. Nanosci. 9 (2010) 151–157.
[17] A.K. Nair, S.W. Cranford, M.J. Buehler, The minimal nanowire: mechanical properties of carbyne, EPL-Europhys. Lett. 95 (2011) 16002.
[18] M. Liu, V.I. Artyukhov, H. Lee, F. Xu, B.I. Yakobson, Carbyne from first principles: chain of C atoms, a nanorod or a nanorope, ACS Nano. 7 (2013) 10075–10082.
[19] X. Liu, G. Zhang, Y.W. Zhang, Tunable mechanical and thermal properties of one-dimensional carbyne chain: phase transition and microscopic dynamics, J. Phys. Chem. C 119 (2015) 24156–24164.
[20] R. Mirzaeifar, Z. Qin, M.J. Buehler, Tensile strength of carbyne chains in varied chemical environments and structural lengths, Nanotechnology 25 (2014) 371001.
[21] S.J. Stuart, A.B. Tutein, J.A. Harrison, A reactive potential for hydrocarbons with intermolecular interactions, J. Chem. Phys. 112 (2000) 6472–6486.
[22] A.K. Ott, G.A. Rechtsteiner, C. Felix, O. Hampe, M.F. Jarrold, R.P. Van Duyne, K. Raghavachari, Raman spectra and calculated vibrational frequencies of size-selected C16, C18, and C20 clusters, J. Chem. Phys. 109 (1998) 9652–9655.
[23] D. Tománek, M.A. Schluter, Growth regimes of carbon clusters, Phys. Rev. Lett. 67 (1991) 2331–2334.
[24] R.O. Jones, G. Seifert, Structure and bonding in carbon clusters C 14 to C 24: chains, rings, bowls, plates, and cages, Phys. Rev. Lett. 79 (1997) 443–446.
[25] Z. Qi, F. Zhao, X. Zhou, Z. Sun, H.S. Park, H. Wu, A molecular simulation analysis of producing monatomic carbon chains by stretching ultranarrow graphene nanoribbons, Nanotechnology 21 (2010) 265702.
[26] Y. Wang, Z.Z. Lin, W. Zhang, J. Zhuang, X.J. Ning, Pulling long linear atomic chains from graphene: molecular dynamics simulations, Phys. Rev. B 80 (2009) 308–310.
[27] X. Yang, Y. Huang, L. Wang, B. Cao, A.C. To, Formation of single carbon chain bridging two SWCNTs via tensile deformation of nanobud junction, Mater. Des. 97 (2016) 86–92.
[28] O. Hod, J.E. Peralta, G.E. Scuseria, Edge effects in finite elongated graphene nanoribbons, Phys. Rev. B 76 (2007) 4692.
[29] H. Zhao, N.R. Aluru, Temperature and strain-rate dependent fracture strength of graphene, J. Appl. Phys. 108 (2010) 064321.
[30] S.J. Plimpton, Fast parallel algorithms for short-range molecular dynamics, J. Comput. Phys. 117 (1993) 1–19.
[31] F. Ma, Y.J. Sun, D.Y. Ma, et al., Reversible phase transformation in graphene nanoribbons: lattice shearing based mechanism, Acta Mater. 59 (2011) 6783–6789.
[32] M. Becton, L. Zhang, X. Wang, On the crumpling of polycrystalline graphene by molecular dynamics simulation, Phys. Chem. Chem. Phys. 17 (2015) 6297–6304.
[33] X. Yang, L. Wang, Y. Huang, Z. Han, A.C. To, Carbon nanotube–fullerene hybrid nanostructures by C 60 bombardment: formation and mechanical behavior, Phys. Chem. Chem. Phys. 16 (2014) 21615–21619.
[34] X. Yang, L. Wang, Y. Huang, Z. Han, A.C. To, B.Y. Cao, Effects of nanobuds and heat welded nanobuds chains on mechanical behavior of carbon nanotubes, Com. Mater. Sci. 109 (2015) 49–55.
[35] L. Xu, X. Zhang, Y. Zheng, Local strain effect on the thermal transport of graphene nanoribbons: a molecular dynamics investigation, Phys. Chem. Chem. Phys. 17 (2015) 12031–12040.
[36] C.M. Shumeyko, E.B. Webb, A molecular dynamics study of lithium grain boundary intercalation in graphite, Scr. Mater. 102 (2015) 43–46.
[37] D.W. Brenner, Empirical potential for hydrocarbons for use in simulating the chemical vapor deposition of diamond films, Phys. Rev. B 42 (1990) 9458–9471.
[38] D.W. Brenner, O.A. Shenderova, J.A. Harrison, S.J. Stuart, B. Ni, S.B. Sinnott, A second-generation reactive empirical bond order (REBO) potential energy expression for hydrocarbons, J. Phys.-Condens. Mater. 14 (2002) 783–802.
[39] H. Li, F.W. Sun, Y.F. Li, X.F. Liu, K.M. Liew, Theoretical studies of the stretching behavior of carbon nanowires and their superplasticity, Scr. Mater. 59 (2008) 479–482.
[40] M. Becton, L. Zhang, X. Wang, Mechanics of graphyne crumpling, Phys. Chem. Chem. Phys. 16 (2014) 18233–18240.
[41] J. Zhao, N. Wei, Z. Fan, J.W. Jiang, T. Rabczuk, The mechanical properties of three types of carbon allotropes, Nanotechnology 24 (2013) 095702–095712.
[42] M. Hu, Y. Jing, X. Zhang, Low thermal conductivity of graphyne nanotubes from molecular dynamics study, Phys. Rev. B 91 (2015) 155408.
[43] Y. Yang, X. Xu, Mechanical properties of graphyne and its family–A molecular dynamics investigation, Com. Mater. Sci. 61 (2012) 83–88.
[44] T. Belytschko, S.P. Xiao, G.C. Schatz, R.S. Ruoff, Atomistic simulations of nanotube fracture, Phys. Rev. B 65 (2002) 235430.
[45] O.A. Shenderova, D.W. Brenner, A. Omeltchenko, X. Su, L.H. Yang, Atomistic modeling of the fracture of polycrystalline diamond, Phys. Rev. B 61 (2000) 3877–3888.
[46] M. Huhtala, A.V. Krasheninnikov, J. Aittoniemi, S.J. Stuart, K. Nordlund, K. Kaski, Improved mechanical load transfer between shells of multiwalled carbon nanotubes, Phys. Rev. B 70 (2004) 2199–2208.
[47] M. Daly, C.V. Singh, A kinematic study of energy barriers for crack formation in graphene tilt boundaries, J. Appl. Phys. 115 (2014) 223513.
[48] J. Gu, F. Sansoz, Role of cone angle on the mechanical behavior of cup-stacked carbon nanofibers studied by atomistic simulations, Carbon 66 (2014) 523–529.
[49] R. Grantab, V.B. Shenoy, R.S. Ruoff, Anomalous strength characteristics of tilt grain boundaries in graphene, Science 330 (2010) 946–948.
[50] Y. Chu, R. Tarek, B. Cemal, The size effect in mechanical properties of finite-sized graphene nanoribbon, Comput. Mater. Sci. 81 (2014) 269–274.
[51] M.A.N. Dewapriya, A. Srikantha Phani, R.K.N.D. Rajapakse, Influence of temperature and free edges on the mechanical properties of graphene, Model. Simul. Mater. Sci. 21 (2013) 2848–2855.
[52] H. Zhao, K. Min, N.R. Aluru, Size and chirality dependent elastic properties of graphene nanoribbons under uniaxial tension, Nano Lett. 9 (2009) 3012–3015.
[53] Y. Zheng, L. Xu, Z. Fan, N. Wei, Z. Huang, A molecular dynamics investigation of the mechanical properties of graphene nanochains, J. Mater. Chem. 22 (2012) 9798–9805.
[54] Y.H. Hu, Bending effect of sp-hybridized carbon (carbyne) chains on their structures and properties, J. Phys. Chem. C 115 (2011) 1843–1850.
[55] Y. Li, L. Xu, H. Liu, Y. Li, Graphdiyne and graphyne: from theoretical predictions to practical construction, Chem. Soc. Rev. 43 (2014) 2572–2586.
[56] H.C. Bai, Y. Zhu, W.Y. Qiao, Y.H. Huang, Structures, stabilities and electronic properties of graphdiyne nanoribbons, RSC Adv. 1 (2011) 768–775.
[57] Y. Pei, Mechanical properties of graphdiyne sheet, Physica B 407 (2012) 4436–4439.
[58] K. Mylvaganam, L.C. Zhang, Important issues in a molecular dynamics simulation for characterising the mechanical properties of carbon nanotubes, Carbon 42 (2004) 2025–2032.
[59] W.C. Liu, F.Y. Meng, S.Q. Shi, A theoretical investigation of the mechanical stability of single- walled carbon nanotube 3-D junctions, Carbon 48 (2010) 1626–1635.
[60] Y. Huang, J. Wu, K.C. Hwang, Thickness of graphene and single-wall carbon nanotubes, Phys. Rev. B 74 (2006) 4070–4079.
[61] O.A. Shenderova, V.V. Zhirnov, D.W. Brenner, Carbon nanostructures, Crit. Rev. Solid State 27 (2002) 227–356.
[62] T. Vodenitcharova, L.C. Zhang, Effective wall thickness of a single-walled carbon nanotube, Phys. Rev. B 68 (2003) 202–206.
[63] S. Cranford, D. Sen, M.J. Buehler, Meso-origami: folding multilayer graphene sheets, Appl. Phys. Lett. 95 (2009) 123121.
[64] Y.J. Sun, Y.H. Huang, F. Ma, D.Y. Ma, T.W. Hu, K.W. Xu, Molecular dynamics simulation on double-elastic deformation of zigzag graphene nanoribbons at low temperature, Mater. Sci. Eng. B 180 (2014) 1–6.
[65] B.I. Yakobson, C.J. Brabec, J. Bernholc, Nanomechanics of carbon tubes: instabilities beyond linear response, Phys. Rev. Lett. 76 (1996) 2511.
[66] A. Timoshevskii, S. Kotrechko, Y. Matviychuk, Atomic structure and mechanical properties of carbyne, Phys. Rev. B 91 (2015) 24535.
[67] S. Kotrechko, A. Timoshevskii, E. Kolyvoshko, Y. Matviychuk, Relation between the strength and dimensionality of defect-free carbon crystals, Nanoscale Res. Lett. 10 (2015) 1–5.
[68] A. Monari, S. Evangelisti, Finite-size Effects in Graphene Nanostructures, INTECH Open Access Publisher, 2011.
[69] S. Ji-rong, W. Yu-nian, P. Fu-cho, Specific heat of a Heisenberg system with finite size, Acta Phys. Sin.-Ch. Ed. 4 (1995) 542–549.
[70] S. Maruyama, A molecular dynamics simulation of heat conduction in finite length SWNTs, Physica B 323 (2002) 193–195.